Ten channel single-mode wavelength division demultiplexer in near IR

Ray T. Chen, Huey Lu, Dan Robinson, and Michael R. Wang

Physical Optics Corporation
2545 West 237th Street, Suite B
Torrance, California 90505

A ten-channel single-mode wavelength division demultiplexer operating at 740, 750, 760, 770, 780, 790, 800, 810, 820 and 830 nm with diffraction angles varying from 16° to 52° and using a graded index (GRIN) polymer waveguide is reported for the first time. Diffraction efficiency up to 60% was measured. The wavelength spreading of the Ti:Al_2O_3 laser (~ 4 nm, 3 dB bandwidth) causes an average crosstalk figure of -21 dB. The beamwidth of the diffracted signal as a function of the input beam width, the grating interaction length, and the diffraction angle are considered. Occurrence of maximum values are discussed. A waveguide lens is needed to efficiently couple the diffracted light into an output fiber whenever the diffracted beam size is beyond the core diameter of the fiber involved.

Wavelength division multiplexing (WDM) and demultiplexing (WDDM) devices have been under intensive research for the past 15 years. Many WDMs and WDDMs that use absorption and/or interference filters [1,2] and diffraction gratings [3-6] have been reported. Wavelength division multiplexing and demultiplexing is a promising technique for both optical communication and sensing systems. Multiplexing an array of signal carriers with different optical frequencies greatly enhances the transmission capacity and the application flexibility of an optical communication system. The dispersion characteristic of the diffraction grating provides an opportunity to employ WD(D)M devices for optical encoders [7,8] to detect both linear and rotational positions. We have developed four-channel visible (543, 594.1, 611.9 and 932.8 nm) [9] and five-channel near IR (730, 750, 780, 810 and 840 nm) [10] single-mode wavelength division demultiplexers using a graded index (GRIN) polymer waveguide in conjunction with a highly multiplexed waveguide hologram. Due to the index tunability of the polymer guide, the reported device can be implemented on an array of substrates.[11-13]

In this paper, we are presenting for the first time a ten-channel single-mode waveguide WDDM with diffraction efficiency as high as 60% and crosstalk of -21 dB. The center wavelengths of these channels are located at 740, 750, 760, 770, 780, 790, 800, 810, 820 and 830 nm. To construct a highly multiplexed waveguide hologram, ten channels in this case, the dispersion of the polymeric material was first determined within the wavelength of interest. The phase-matching condition associated with each grating and the corresponding diffracted beam can be constructed afterwards. Note that the isotropic characteristic of the polymer thin film significantly eases the fabrication of the associated diffraction gratings. Anisotropic diffraction is eliminated in this case. For each fixed wavelength λ_j, the associated diffraction angle θ_j is given by

$$\theta_j = 2 \sin^{-1}\left(\frac{\lambda_j}{2 N_{eff_j} \Lambda_j}\right) \qquad (1)$$

Here Λ_j is the grating spacing and N_{eff_j} is the effective index of the polymer waveguide at wavelength λ_j. To precisely control the Bragg diffraction angle θ_j, $N_{eff}(\lambda)$ has to be measured before hologram formation. Coating thickness and dry and wet processing conditions have to be standardized to validate the design process. To fabricate a waveguide hologram with a desired grating spacing, a well-collimated beam is introduced onto the waveguide emulsion containing the hologram.[14] The object and reference

8194-0714-3/91/$4.00

beams require a very short temporal coherence length of the laser beam. For each θ_j, two rotational angles φ_j and w_j, which control the value of Λ_j and the diffraction angle θ_j, respectively, are selected for the waveguide hologram such that

$$\varphi_j = \cos^{-1}\left(\frac{\lambda_R}{2\,\Lambda_j}\right) \tag{2}$$

and

$$w_j = 0.5\,(\pi - \theta_j) \tag{3}$$

can be satisfied simultaneously. In Eq. (2), λ_R is the recording wavelength. The size of the collimated beam is much larger than the interaction length (submillimeter), i.e., grating thickness (Figure 1) of the waveguide. As a result, each waveguide hologram is formed by two plane waves. For a perfectly phase-matched, lossless, unslanted transmission grating, the diffraction efficiency can be written as [15]

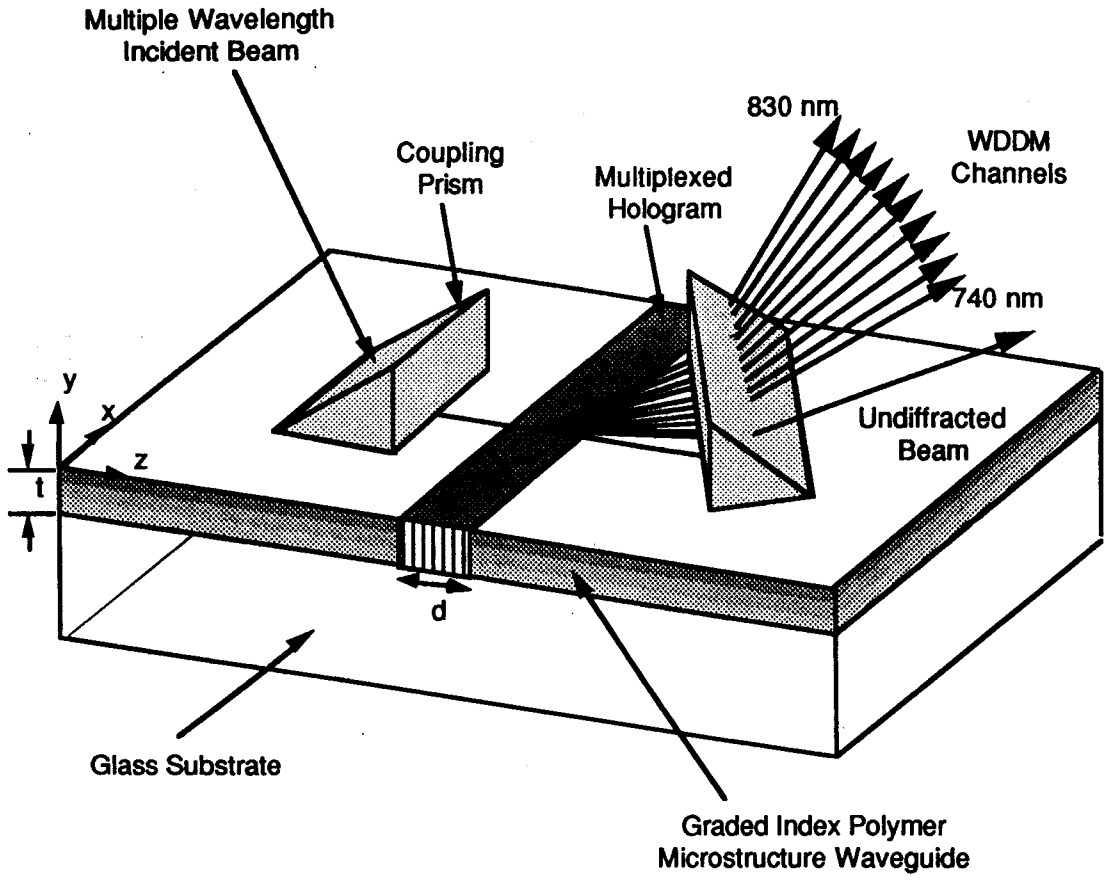

Figure 1 Reconstruction of the waveguide WDDM device using a Ti:Al_2O_3 laser.

$$\eta_j = \sin^2\left(\frac{\pi \Delta n_j d}{\lambda_j \cos\theta_j}\,\xi\right) \tag{4}$$

where Δn_j and d are the associated index modulation and the interaction length, respectively, and ξ is a constant which varies between 0 and 1 depending on the polarization of the incident beam.[12] The recording setup for fabricating a highly multiplexed hologram is shown in Figure 2. The sinusoidal nature of the device requires precise control of θ_j, Δn_j and d in order to generate a highly multiplexed hologram with uniform fan-out intensity. d is controlled by the lithographic process and Δn is manipulated through exposure dosage and wet and dry processing parameters. To introduce the desired index modulation, the exposure time t_j needed for the jth hologram should satisfy the following equation[15]

$$t_j = \frac{1}{E\beta} \ln\left[-\Delta n_j + \left(\Delta n_{max} - \sum_{i=1}^{j-1} \Delta n_i\right)\right] \Big/ \left[\Delta n_{max} - \sum_{i=1}^{j-1} \Delta n_i\right] \tag{5}$$

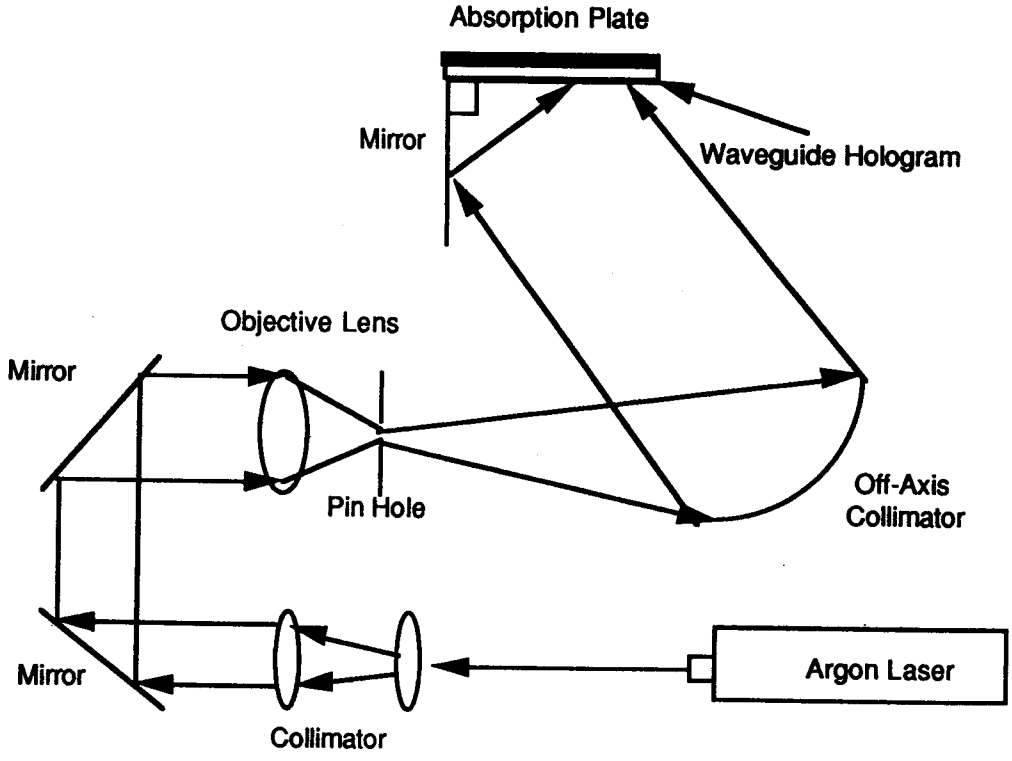

Figure 2 Waveguide hologram recording setup.

where β is the sensitivity constant for the emulsion, E is the exposure intensity of the laser beam, Δn_i is the index modulation for the ith exposure and Δn_{max} is the maximum index modulation for the holographic material. Note that the exposure dosage needed to generate a fixed value of index modulation increases as the number of holograms to be multiplexed increases. This is due to the fixed

value of Δn_{max} and the linear response of the film. Eq. (5) has been experimentally confirmed and further results will be presented in the future. For the present WDDM device, the gratings were designed to operate at the diffraction angles of 16°, 20°, 24°, 28°, 32°, 36°, 40°, 44°, 48° and 52° to selectively disperse signals at the center wavelengths of 740, 750, 760, 770, 780, 790, 800, 810, 820 and 830 nm, respectively. For each λ_j, the corresponding φ_j and w_j were selected to generate a waveguide transmission hologram with the desired Λ_j and θ_j. Figure 1 shows the reconstruction of the waveguide WDDM device using Ti:Al_2O_3 laser light as the input signal. The interaction length of the multiplexed waveguide hologram is 0.33 mm. The mode dots coupled out of the prism coupler are shown in Figures 3(a) and 3(b) with the corresponding wavelengths as indicated in Figure 3(b). The observation of these clean mode dots verified the quality of the polymer waveguide. A propagation loss of less than 0.5 dB/cm has been routinely achieved in a Class 100 clean room environment. As was previously reported, the channel density [13] of the WDDM device is a function of Δn_j, d and θ_j. The correlation of these parameters can also be observed in Eq. (4). A higher index modulation and longer interaction length provide us with narrower FMHW (full width at half maximum) diffraction spreading and, thus, higher channel density. With an incident beamwidth of Ω, the beamwidth δ of the associated diffracted beam is a function of Ω, d and θ_j. The computer-simulated results with Ω = 100 μm are further illustrated in Figure 4(a) where d varies from 10 μm to 500 μm and θ_j swings from 0° to 90°. The maximal value of δ occurs, when [16]

$$\theta_j = \tan^{-1}\frac{d}{\Omega} \tag{6}$$

It is obvious from Figure 4(a) and Eq. (6) that the maximum δ value shifts to larger diffraction angles as the interaction length increases. In order to pigtail with an output fiber, the spot size should be well-matched with the core diameter of the fiber. Figure 4(b) shows the contour lines of equal spot size for the diffracted beam. Contour lines corresponding to 50, 75, 100, 125 μm, etc., are clearly indicated. It is obvious from the preceding discussion that there is a tradeoff between the channel density and the value of δ (d, Ω, θ_j) over which a number of diffracted lights with different wavelengths can be efficiently coupled into the fiber array. With a δ value larger than the core diameter of the output fiber, a focusing lens array is needed to provide high coupling efficiency. Locally sensitized holographic emulsion can be employed for this purpose. Both holographic lenses produced by two-beam interference and contact printing lenses produced by optical lithography based on the waveguide holographic material reported here can be fabricated. Recently, polymer waveguide lenses on Si and GaAs have been successfully demonstrated. The noise of the fan-out channels of the WDDM device is mainly from the crosstalk of the signals from adjacent channels. An average crosstalk figure of -21 dB was measured with diffraction efficiency from 52% to 60% among these output channels (Figure 5). The spectral width of the Ti:Al_2O_3 laser from Spectrophysics was also measured. A -3 dB bandwidth of ~4 nm was found. The results suggest that the WDM devices of better than 4 nm wavelength separation cannot be experimentally realized without significant channel crosstalk. Theoretically, our device structure is capable of operating at a channel-to-channel spacing as small as 1 nm under the current design, when a DFB laser diode is employed. The -21 dB crosstalk is primarily due to the wavelength spreading of the Ti:Al_2O_3 laser rather than the waveguide device itself.

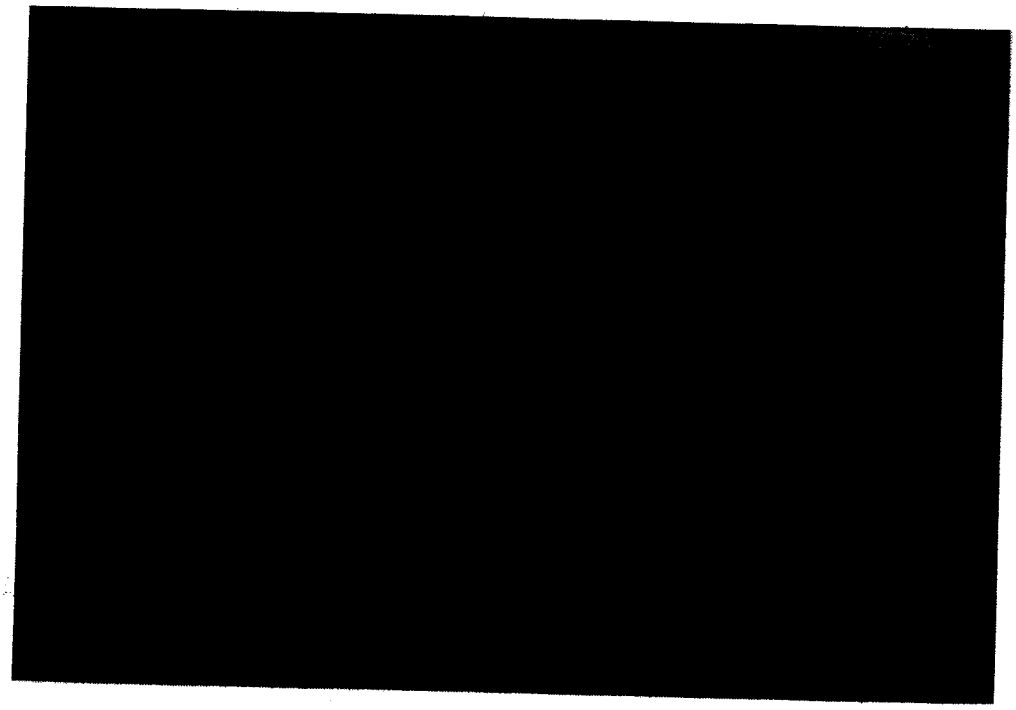

(a)

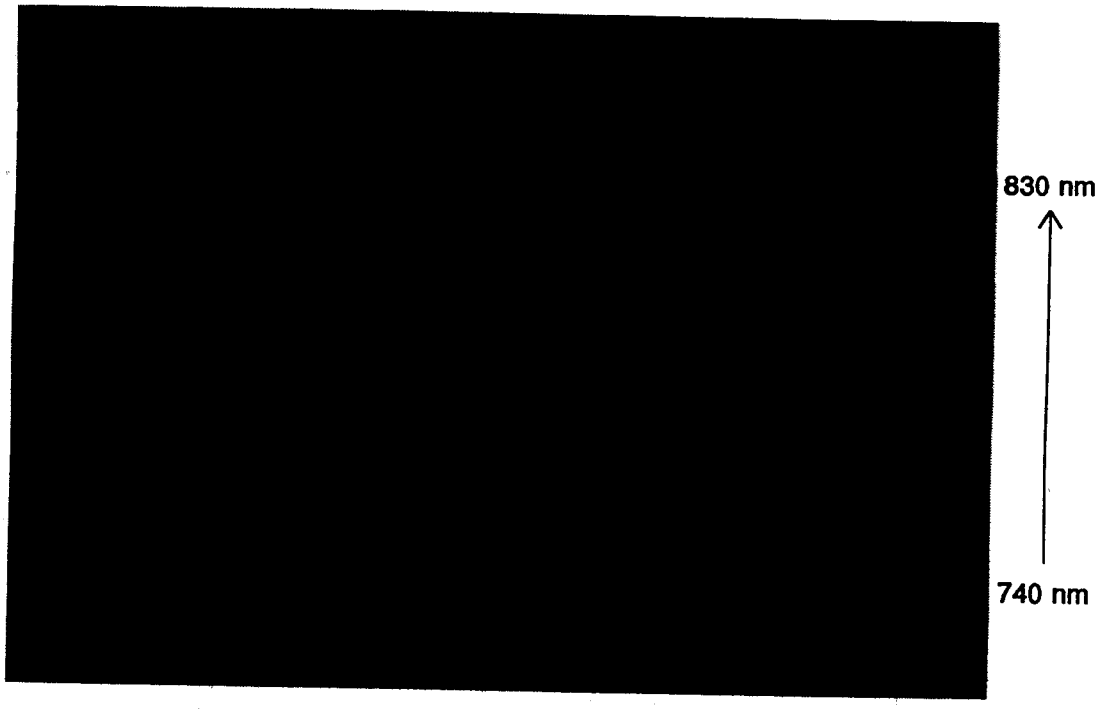

(b)

Figure 3 (a) 1-to-10 WDDM device working at near IR and (b) mode dots from the output prism coupler (Figure 2) of the 10-channel WDDM.

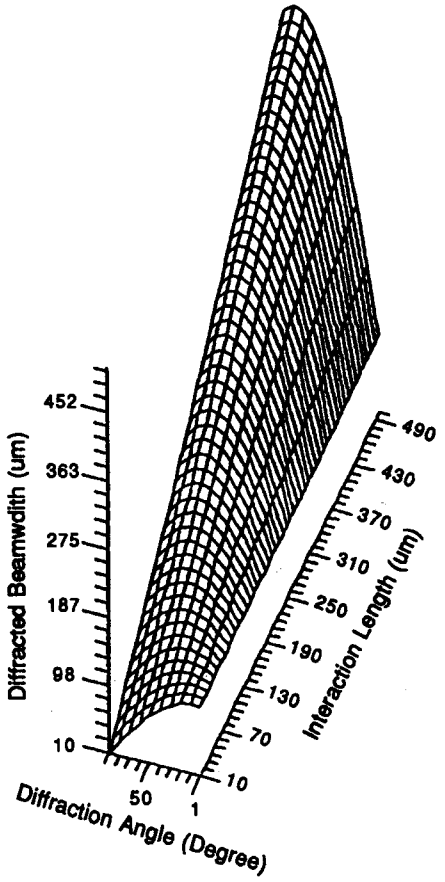

(a)

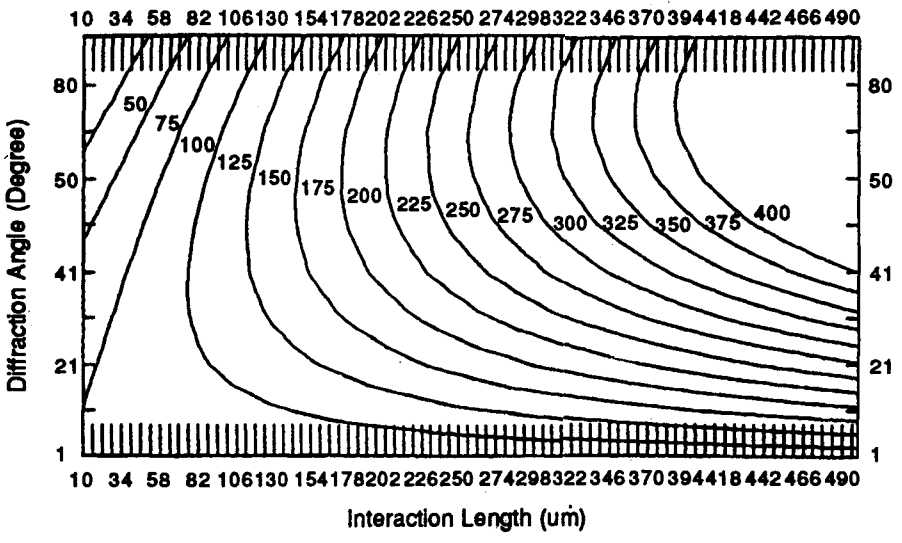

(b)

Figure 4 Diffracted beamwidth (a) as a function of grating interaction length and diffraction angle with $\Omega = 100$ μm and (b) equal beamwidth line topology.

The current design allows us to provide 120-channel multiplexibility with the maximum value of index modulation set at 0.2. We report a single-mode, GRIN-polymer-based waveguide WDDM device. Ten-channel WDDM (740, 750, 760, 770, 780, 790, 800, 810, 820, and 830 nm) with channel separation of 4° in space and 10 nm in wavelength has been demonstrated with an average crosstalk figure of -21 dB. The spreading of the Ti:Al_2O_3 laser turned out to be the major source of crosstalk from adjacent channels. Theoretically, WDDM channel spacing as small as 1 nm is plausible under the current design criterion. To understand the effect of finite beam size and interaction length, the diffracted beam spot size was also considered. The variation of beam spot size as a function of diffraction angle and grating interaction length with 100 μm input beamwidth is presented here. A diffraction spot whose beamwidth is larger than that of its output fiber requires the implementation of a waveguide lens array to enhance the coupling efficiency. Further results on waveguide lens arrays will be presented in the future.

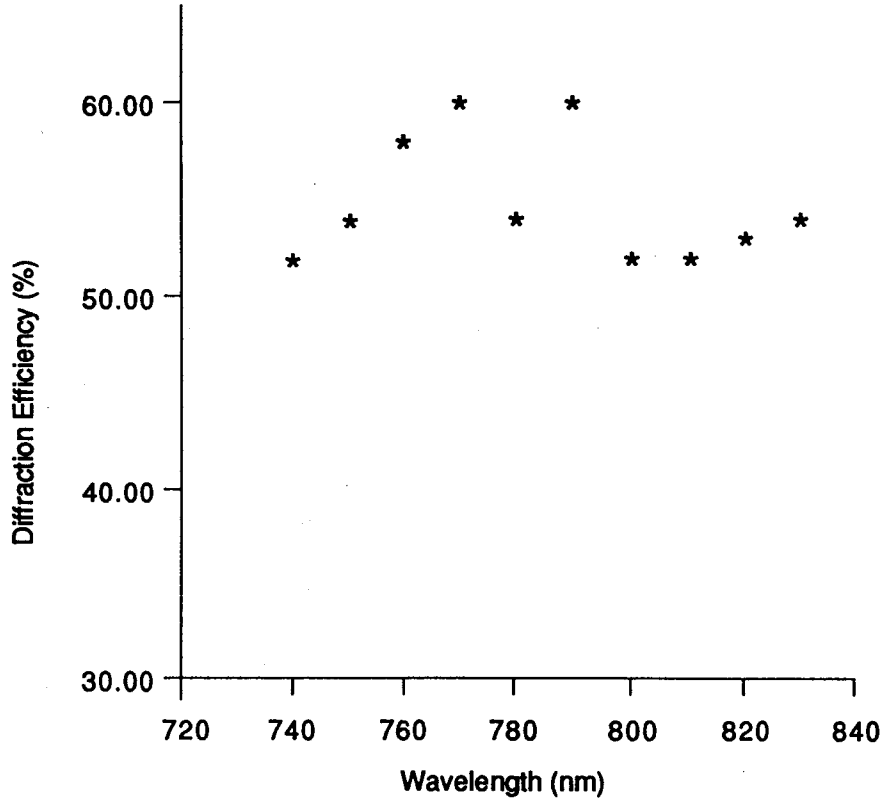

Figure 5 Diffraction efficiency of a 10-channel WDDM. (The 52% channel represents ~70 mW diffracted power.)

The device reported here not only enhances the bandwidth of optical interconnects but also provides us with a new avenue through which dispersion-sensitive optical sensors, such as optical encoders,[7] can be realized. The GRIN property of the polymer waveguide allows us to implement the reported device on an array of substrates. Such universality greatly enhances the application scenarios in which conventional guided wave devices can be used.

REFERENCES

1. I. Bennion, D. C. Reid, C. J. Rowe, and W. J. Stewart, *Electron. Lett.*, vol. 22, p. 341, 1986.
2. W. V. Sorin, P. Zorahedian, and S. A. Newton, *IEEE J. Lightwave Tech.*, vol. LT-5, no. 9, p. 1199, 1987.
3. K. Kobayashi and M. Seki, *IEEE J. Quantum Electron.*, vol. QE-16, no. 1, p. 11, 1980.
4. S. Ura, M. Morisawa, T. Suhara, and H. Nishihara, *Appl. Opt.*, vol. 29, no. 9, p. 1369, 1990.
5. Y. Fujii, J. Minowa, and Y. Yamada, *IEEE J. Lightwave Technology*, vol. LT-2, no. 5, p. 731, 1984.
6. T. Von Lingelsheim, *IEEE Proc.*, vol. 131, no. 5, p. 290, 1984.
7. R. T. Chen, M. R. Wang, G. Sonek, and T. Jannson, *Opt. Eng.*, vol. 30, p. 622, 1991.
8. D. W. Seal, Final Report to NASA, Contract. No. NAS3-25345, 1989.
9. M. R. Wang, R. T. Chen, G. Sonek, and T. Jannson, *Opt. Lett.*, vol. 15, p. 363, 1990.
10. M. R. Wang, G. Sonek, R. T. Chen, and T. Jannson, *IEEE Photonics Technology Letters*, vol. 3, p. 36, 1991.
11. R. T. Chen, W. Phillips, T. Jannson, and D. Pelka, *Opt. Lett.*, vol. 14, p. 892, 1989.
12. R. T. Chen, M. R. Wang, and T. Jannson, *Appl. Phys. Lett.*, vol. 56, p. 709, 1990.
13. R. T. Chen, *Proc. SPIE*, vol. 1374, p. 20, 1990.
14. R. T. Chen, M. R. Wang, F. Lin, and T. Jannson, *Proc. SPIE*, vol. 1213, p. 27, 1991.
15. R. T. Chen, M. R. Wang, and T. Jannson, *Appl. Phys. Lett.*, vol. 57, p. 2071, 1990.
16. R. T. Chen, H. Lu, and T. Jannson, Topical Meeting on Gradient-Index Optical Systems, Technical Digest Series, (Optical Society of America, Washington, DC 1991), PD2-1.